Cooling by Coulomb Heat Drag Based on Three Coupled Quantum Dots

Jin-Zhu Gao(高金柱), Xing Liu(刘行), Jian-Hui Wang(王建辉), and Ji-Zhou He(何济洲)*

Department of Physics, Nanchang University, Nanchang 330031, China

(Received 29 June 2023; accepted manuscript online 25 September 2023)

We establish a model for a four-terminal thermoelectric system, based on three coupled quantum dots, which consists of a left/right electron reservoir (the source and the drain), two thermal reservoirs and three coupled quantum dots. Based on the master equation theory, we derive the expressions of the electron current and heat flow among the three quantum dots and the corresponding reservoir. We show that the source can be cooled by passing a thermal current between the two thermal reservoirs, with no net heat exchange between the thermal reservoirs and the electron reservoirs. This effect is called the Coulomb heat drag effect. Then, we define the coefficient of performance (COP) and the cooling power. The influence of the main system parameters, such as charging energy, energy level, and temperature, on the performance of the four-terminal thermoelectric system is analyzed in detail. By choosing appropriate parameters one can obtain the maximum cooling power and the corresponding COP. Finally, we also show that the Maxwell demon effect can be realized by using nonequilibrium thermal reservoirs in our four-terminal thermoelectric system.

DOI: 10.1088/0256-307X/40/11/117301

There are currently great interests in quantum and nanoscale systems that convert heat into electricity as a heat engine using the Seebeck effect or convert electricity into heat as a refrigerator using the Peltier effect. These systems include quantum dots and a quantum well,[1–5] nanowire and a superlattice,[6,7] etc.[8–13] Configuration aspects include two-terminal, three-terminal or four-terminal thermoelectric devices. Compared to conventional two-terminal thermoelectric devices, three-terminal thermoelectric devices can improve the thermodynamic performance significantly by separating the electron current and heat current, including electron–phonon or electron–electron interaction, electron–photon or electron–magneton interaction.[14–29]

For example, Sánchez *et al.* first proposed a three-terminal energy convertor based on two capacitively coupled quantum dots in the Coulomb-blockade regime in 2011. It can generate electricity by investing thermal power from a hot reservoir and this converter can achieve Carnot efficiency in optimal configuration.[30] A few years later, Thierschmann *et al.* proved this kind of energy convertor's working principle through experiments.[31] Zhang *et al.* proposed a three-terminal quantum-dot refrigerator based on two coupled quantum dots. They also analyzed this kind of refrigerator's thermodynamic performance in detail when some irreversible factors are taken into account.[32] Singha *et al.* proposed a realistic nonlocal heat engine and refrigerator based on a triple quantum dot system and analyzed their thermodynamic performance by using a master equation.[33,34] Significant progress has been made in experimental research on three-terminal nanostructured thermoelectric devices.[35–38]

Current research on four-terminal thermoelectric devices is relatively rare and it is also a relatively new field. Keller *et al.* observed Coulomb drag in a Coulomb-coupled double quantum dot and obtained a correct explanation through both experimental and theoretical arguments.[39] Whitney *et al.* proposed a thermocouple heat engine based on three capacitively coupled quantum dots and it can generate electricity even when the total thermal power invested from two thermal reservoirs is zero.[40] Su *et al.* proposed a thermodynamic pump based on a triple quantum dot system that is driven by Maxwell's demon. They analyzed how the information that drives the mass or heat transfer is generated in the pump by using Markov stochastic thermodynamics.[41] Jiang *et al.* analyzed the cooling by heat current effect that is driven by Coulomb drag in a four-terminal mesoscopic thermoelectric system.[42,43] He *et al.* proposed a four-terminal hybrid drive refrigerator model with three capacitively coupled quantum dots, and compared the performance of this refrigerator in strong and weak capacitive coupling cases.[44] Based on these previous works, in this Letter we propose a four-terminal quantum dot thermoelectric system as a refrigerator with three capacitively coupled quantum dots. The focus in this study is to show the cooling by Coulomb heat drag effect, analyze the thermodynamic performance characteristics of the refrigerator, and demonstrate the Maxwell demon effect.

The model we consider is schematically illustrated in Fig. 1. It consists of a quantum dot $\mathrm{QD_M}$ embedded between left and right electron reservoirs (the source S and the drain D) with temperature $(T_\mathrm{S}, T_\mathrm{D})$ and chemical potential $(\mu_\mathrm{S}, \mu_\mathrm{D})$, and the other two quantum dots $\mathrm{QD_H}$ and $\mathrm{QD_C}$ connected to a high-temperature thermal reservoir with temperature T_H, chemical potential μ_H, low-

*Corresponding author. Email: hjzhou@ncu.edu.cn

© 2023 Chinese Physical Society and IOP Publishing Ltd

temperature thermal reservoir with temperature $T_{\rm C}$ and chemical potential $\mu_{\rm C}$, respectively. The temperature $T_{\rm S}$ of the source is lower than the temperature $T_{\rm D}$ of the drain. Three quantum dots $\rm QD_M$, $\rm QD_H$, and $\rm QD_C$ are coupled to each other and they interact with each other through long-range Coulomb interaction. The Coulomb charging energies are denoted by $U_{\rm MH}$, $U_{\rm MC}$, and $U_{\rm HC}$. If the quantum dots are far from each other, they can be bridged to obtain a strong/weak coupling and at the same time ensure good thermal isolation between the electron reservoir and the thermal reservoir.

Three quantum dots $\rm QD_M$, $\rm QD_H$, and $\rm QD_C$ have their respective single energy levels $\varepsilon_{\rm M}$, $\varepsilon_{\rm H}$ and $\varepsilon_{\rm C}$. The quantum states of this triple-dot system are expressed as (m, h, c), with m, h, and c being the electron occupation numbers of the respective quantum dots $\rm QD_M$, $\rm QD_H$, and $\rm QD_C$. Since Coulomb interaction prevents two electrons from being present at one energy level at the same time, the single energy level $\varepsilon_{\rm M}$, $\varepsilon_{\rm H}$, or $\varepsilon_{\rm C}$ can be occupied only by zero or one electron. Therefore, there are eight quantum states in this system. They are denoted as $(0,0,0)$, $(1,0,0)$, $(0,1,0)$, $(0,0,1)$, $(1,1,0)$, $(1,0,1)$, $(0,1,1)$, and $(1,1,1)$. The dynamical processes of the quantum states are shown in Fig. 2, where $[\Gamma_\alpha]^{m'h'c'}_{mhc}$ represents the transition rate of the three-dot system from state (m', h', c') to state (m, h, c) due to electron tunneling into or out of reservoir α ($\alpha = \rm S, D, H, C$). When the tunneling events in these sequences involve an electron that tunnels from reservoir S into the dot, and thereafter into reservoir D (or vice versa), it contributes to the transport process. For example, one cycle is $(0,0,0) \to (1,0,0) \to (1,1,0) \to (0,1,0) \to (0,0,0)$, and the other is $(0,0,0) \to (1,0,0) \to (1,0,1) \to (0,0,1) \to (0,0,0)$.

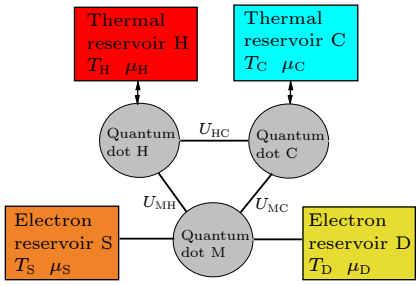

Fig. 1. Schematic diagram of a four-terminal quantum dot thermoelectric system.

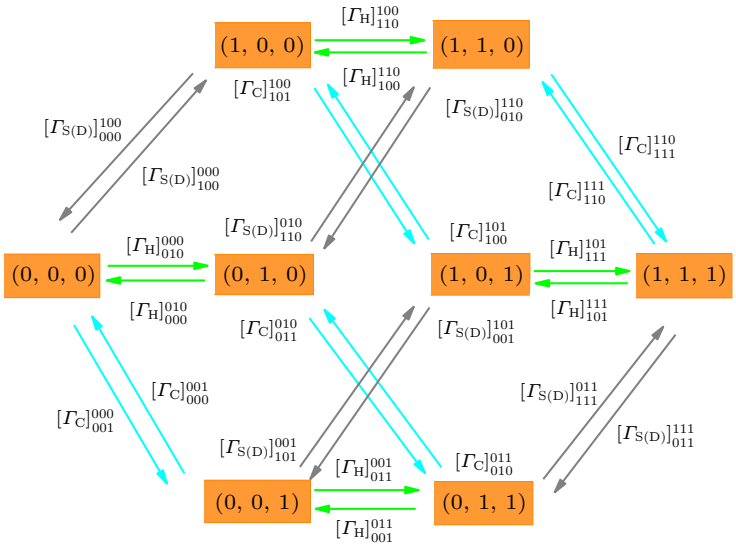

Fig. 2. Dynamic processes of the quantum states.

In sequential tunneling approximation ($\hbar\gamma \ll k_{\rm B}T$), the energy level width of the quantum dot can be ignored, and the electron transport process is defined as sequential tunneling. Therefore, the dynamical evolution of the occupation probability of quantum states with time is described by the master equation

$$\dot{P}_{mhc} = \sum_{m'h'c'} [M]^{m'h'c'}_{mhc} P_{m'h'c'}, \tag{1}$$

with $\sum_{mhc} P_{mhc} = 1$. Here, P_{mhc} represents the probability of state (m, h, c). All non-diagonal elements of the transition matrix are determined by $[M]^{m'h'c'}_{mhc} = \sum_{\alpha=\rm S,D,H,C} [\Gamma_\alpha]^{m'h'c'}_{mhc}$, namely by the sum over the transition rates of the three-dot system from state (m', h', c') to state (m, h, c). The latter is given by $[\Gamma_\alpha]^{m'h'c'}_{mhc} = [\gamma_\alpha]^{m'h'c'}_{mhc} f_\alpha(\Delta^{m'h'c'}_{mhc})$, where $[\gamma_\alpha]^{m'h'c'}_{mhc}$ is the bare tunneling rate of the system from state (m', h', c') to state (m, h, c) between the quantum dot and the corresponding reservoirs α, $f_\alpha(x) = 1/(1 + e^{(x-\mu_\alpha)/k_{\rm B}T_\alpha})$ is the Fermi function that describes the electron distribution of reservoir α with chemical potential μ_α and temperature T_α, $\Delta^{m'h'c'}_{mhc} = E_{mhc} - E_{m'h'c'}$, E_{mhc} is the energy of the quantum state (m, h, c), and $k_{\rm B}$ is the Boltzmann constant. The diagonal elements in Eq. (1) are directly found by using the condition that every column of the transition matrix sums to zero to fulfill probability conservation, $[M]^{mhc}_{mhc} = -\sum_{mhc \neq m'h'c'} [M]^{m'h'c'}_{mhc}$.

Based on Eq. (1), in the steady state, i.e., $\dot{P}_{mhc} = 0$,

we can obtain the solution of the occupation probability P_{mhc} of each quantum state (m, h, c). The electron current from the source S to the quantum dot $\mathrm{QD_M}$ is given by

$$\begin{aligned} I_{\mathrm{S}} =& [\Gamma_{\mathrm{S}}]^{000}_{100}P_{000} - [\Gamma_{\mathrm{S}}]^{100}_{000}P_{100} + [\Gamma_{\mathrm{S}}]^{010}_{110}P_{010} \\ &- [\Gamma_{\mathrm{S}}]^{110}_{010}P_{110} + [\Gamma_{\mathrm{S}}]^{001}_{101}P_{001} - [\Gamma_{\mathrm{S}}]^{101}_{001}P_{101} \\ &+ [\Gamma_{\mathrm{S}}]^{001}_{111}P_{001} - [\Gamma_{\mathrm{S}}]^{111}_{001}P_{111}, \end{aligned} \tag{2}$$

and the electron current from the drain D to the quantum dot $\mathrm{QD_M}$ is given by

$$\begin{aligned} I_{\mathrm{D}} =& [\Gamma_{\mathrm{D}}]^{000}_{100}P_{000} - [\Gamma_{\mathrm{D}}]^{100}_{000}P_{100} + [\Gamma_{\mathrm{D}}]^{010}_{110}P_{010} \\ &- [\Gamma_{\mathrm{D}}]^{110}_{010}P_{110} + [\Gamma_{\mathrm{D}}]^{001}_{101}P_{001} - [\Gamma_{\mathrm{D}}]^{101}_{001}P_{101} \\ &+ [\Gamma_{\mathrm{D}}]^{001}_{111}P_{001} - [\Gamma_{\mathrm{D}}]^{111}_{001}P_{111}. \end{aligned} \tag{3}$$

In the steady state, the magnitudes of electron currents I_{S} and I_{D} are the same but their directions are opposite, i.e., $I = I_{\mathrm{S}} = -I_{\mathrm{D}}$.

The heat current into the quantum dot $\mathrm{QD_M}$ from the source S is

$$\begin{aligned} J_{\mathrm{S}} =& (\varepsilon_{\mathrm{M}} - \mu_{\mathrm{S}})([\Gamma_{\mathrm{S}}]^{000}_{100}P_{000} - [\Gamma_{\mathrm{S}}]^{100}_{000}P_{100}) \\ &+ (\varepsilon_{\mathrm{M}} + U_{\mathrm{MH}} - \mu_{\mathrm{S}})([\Gamma_{\mathrm{S}}]^{010}_{110}P_{010} - [\Gamma_{\mathrm{S}}]^{110}_{010}P_{110}) \\ &+ (\varepsilon_{\mathrm{M}} + U_{\mathrm{MC}} - \mu_{\mathrm{S}})([\Gamma_{\mathrm{S}}]^{001}_{101}P_{001} - [\Gamma_{\mathrm{S}}]^{101}_{001}P_{101}) \\ &+ (\varepsilon_{\mathrm{M}} + U_{\mathrm{MH}} + U_{\mathrm{MC}} - \mu_{\mathrm{S}}) \\ &\cdot ([\Gamma_{\mathrm{S}}]^{011}_{111}P_{001} - [\Gamma_{\mathrm{S}}]^{111}_{011}P_{111}), \end{aligned} \tag{4}$$

and the heat current into the drain D from the quantum dot $\mathrm{QD_M}$ is

$$\begin{aligned} J_{\mathrm{D}} =& (\mu_{\mathrm{D}} - \varepsilon_{\mathrm{M}})([\Gamma_{\mathrm{D}}]^{000}_{100}P_{000} - [\Gamma_{\mathrm{D}}]^{100}_{000}P_{100}) \\ &+ (\mu_{\mathrm{D}} - \varepsilon_{\mathrm{M}} - U_{\mathrm{MH}})([\Gamma_{\mathrm{D}}]^{010}_{110}P_{010} - [\Gamma_{\mathrm{D}}]^{110}_{010}P_{110}) \\ &+ (\mu_{\mathrm{D}} - \varepsilon_{\mathrm{M}} - U_{\mathrm{MC}})([\Gamma_{\mathrm{D}}]^{001}_{101}P_{001} - [\Gamma_{\mathrm{D}}]^{101}_{001}P_{101}) \\ &+ (\mu_{\mathrm{D}} - \varepsilon_{\mathrm{M}} - U_{\mathrm{MH}} - U_{\mathrm{MC}}) \\ &\cdot ([\Gamma_{\mathrm{D}}]^{011}_{111}P_{001} - [\Gamma_{\mathrm{D}}]^{111}_{011}P_{111}). \end{aligned} \tag{5}$$

The heat current into the quantum dot $\mathrm{QD_H}$ from the high-temperature reservoir H is

$$\begin{aligned} J_{\mathrm{H}} =& (\varepsilon_{\mathrm{H}} - \mu_{\mathrm{H}})([\Gamma_{\mathrm{H}}]^{000}_{010}P_{000} - [\Gamma_{\mathrm{H}}]^{010}_{000}P_{010}) \\ &+ (\varepsilon_{\mathrm{H}} + U_{\mathrm{MH}} - \mu_{\mathrm{H}})([\Gamma_{\mathrm{H}}]^{100}_{110}P_{100} - [\Gamma_{\mathrm{H}}]^{110}_{100}P_{110}) \\ &+ (\varepsilon_{\mathrm{H}} + U_{\mathrm{HC}} - \mu_{\mathrm{H}})([\Gamma_{\mathrm{H}}]^{001}_{011}P_{001} - [\Gamma_{\mathrm{H}}]^{011}_{001}P_{011}) \\ &+ (\varepsilon_{\mathrm{H}} + U_{\mathrm{MH}} + U_{\mathrm{HC}} - \mu_{\mathrm{H}}) \\ &\cdot ([\Gamma_{\mathrm{H}}]^{101}_{111}P_{101} - [\Gamma_{\mathrm{H}}]^{111}_{101}P_{111}), \end{aligned} \tag{6}$$

and the heat current into the low-temperature reservoir C from the quantum dot $\mathrm{QD_C}$ is

$$\begin{aligned} J_{\mathrm{C}} =& (\mu_{\mathrm{C}} - \varepsilon_{\mathrm{C}})([\Gamma_{\mathrm{C}}]^{000}_{001}P_{000} - [\Gamma_{\mathrm{C}}]^{001}_{000}P_{001}) \\ &+ (\mu_{\mathrm{C}} - \varepsilon_{\mathrm{C}} - U_{\mathrm{MC}})([\Gamma_{\mathrm{C}}]^{100}_{101}P_{100} - [\Gamma_{\mathrm{C}}]^{101}_{100}P_{101}) \\ &+ (\mu_{\mathrm{C}} - \varepsilon_{\mathrm{C}} - U_{\mathrm{HC}})([\Gamma_{\mathrm{C}}]^{010}_{011}P_{010} - [\Gamma_{\mathrm{C}}]^{011}_{010}P_{011}) \\ &+ (\mu_{\mathrm{C}} - \varepsilon_{\mathrm{C}} - U_{\mathrm{MC}} - U_{\mathrm{HC}}) \\ &\cdot ([\Gamma_{\mathrm{C}}]^{110}_{111}P_{110} - [\Gamma_{\mathrm{C}}]^{111}_{110}P_{111}). \end{aligned} \tag{7}$$

The whole system follows the law of energy conservation:

$$J_{\mathrm{S}} + J_{\mathrm{H}} - J_{\mathrm{C}} - J_{\mathrm{D}} = (\mu_{\mathrm{D}} - \mu_{\mathrm{S}})I. \tag{8}$$

Thus, out of the four heat currents, i.e., J_{S}, J_{D}, J_{H}, and J_{C}, only three are independent. It is instructive to introduce the following combinations:

$$J_{\mathrm{in}} = J_{\mathrm{H}} - J_{\mathrm{C}}, \tag{9}$$

$$J_{\mathrm{q}} = \frac{1}{2}(J_{\mathrm{H}} + J_{\mathrm{C}}), \tag{10}$$

where J_{in} is the total heat current flowing into dot M from the two thermal reservoirs H and C, and J_{q} is the heat current to transfer from reservoir H to C. Three independent heat currents are chosen as J_{S}, J_{in}, and J_{q}. By analyzing the total entropy production, the affinities corresponding to the three independent heat currents and electrical current can be found as follows:

$$\frac{dS}{dt} = \sum_i J_i A_i, \tag{11}$$

$$A_{\mathrm{e}} = \frac{\mu_{\mathrm{S}} - \mu_{\mathrm{D}}}{eT_{\mathrm{D}}}, \tag{12}$$

$$A_{\mathrm{S}} \equiv \frac{1}{T_{\mathrm{D}}} - \frac{1}{T_{\mathrm{S}}}, \tag{13}$$

$$A_{\mathrm{in}} \equiv \frac{1}{T_{\mathrm{D}}} - \frac{1}{2T_{\mathrm{H}}} - \frac{1}{2T_{\mathrm{C}}}, \tag{14}$$

$$A_{\mathrm{q}} \equiv \frac{1}{T_{\mathrm{C}}} - \frac{1}{T_{\mathrm{H}}}, \tag{15}$$

where the electrical current is $J_{\mathrm{e}} = eI$. Based on the above expressions, the heat current J_{S} is driven by the temperature difference between the source and the drain. The heat current J_{in} is driven by the temperature difference between the drain and the two thermal reservoirs, and the heat current J_{q} is driven by the temperature difference between the two thermal reservoirs.

In order to demonstrate the cooling by Coulomb heat drag effect, we set the scenarios with

$$\mu_{\mathrm{S}} = \mu_{\mathrm{D}} = 0, \quad \text{i.e.,} \quad A_{\mathrm{e}} = 0, \tag{16}$$

$$T_{\mathrm{C}} = \Big[\frac{2}{T_{\mathrm{D}}} - \frac{1}{T_{\mathrm{H}}}\Big]^{-1}, \quad \text{i.e.,} \quad A_{\mathrm{in}} = 0, \tag{17}$$

and $T_{\mathrm{H}} > T_{\mathrm{D}} > T_{\mathrm{C}}$. Cooling by Coulomb heat drag cools the source (i.e. $J_{\mathrm{S}} > 0$, even though $T_{\mathrm{S}} < T_{\mathrm{D}}$ and $A_{\mathrm{S}} < 0$) by the positive heat current J_{q} (since $T_{\mathrm{H}} > T_{\mathrm{C}}$, $A_{\mathrm{q}} > 0$). We set T_{D} as a reference temperature, and T_{H} and T_{S} as two independent variables. Due to the second law of thermodynamics, the total entropy production is non-negative, i.e.,

$$\frac{dS}{dt} = J_{\mathrm{q}}A_{\mathrm{q}} + J_{\mathrm{S}}A_{\mathrm{S}} \geqslant 0. \tag{18}$$

This cooling effect can occur only at $J_{\mathrm{q}}A_{\mathrm{q}} > 0$. This means that the negative entropy production during the cooling of the source ($J_{\mathrm{S}}A_{\mathrm{S}} < 0$) is compensated for by the positive entropy production during the heat transfer process between two thermal reservoirs ($J_{\mathrm{q}}A_{\mathrm{q}} > 0$).

The coefficient of performance (COP) for the cooling by Coulomb heat drag effect in our four-terminal thermoelectric system is defined by the ratio of the two heat currents:

$$\eta_{\mathrm{COP}} = \frac{J_{\mathrm{S}}}{J_{\mathrm{q}}}. \tag{19}$$

Based on Eq. (18) and the definition of the COP, a reversible COP is

$$\eta_{\rm COP}^{\rm rev} = \left(\frac{T_{\rm S}}{T_{\rm C}} - \frac{T_{\rm S}}{T_{\rm H}}\right)\frac{T_{\rm D}}{T_{\rm D} - T_{\rm S}} = -\frac{A_{\rm q}}{A_{\rm S}}. \tag{20}$$

In the reversible case, the COP is maximum and the cooling power disappears because the entropy production and the currents vanish.[45] The working regions of the cooling driven by the thermal current $J_{\rm q}$ are

$$0 < \eta_{\rm COP} < -\frac{A_{\rm q}}{A_{\rm S}}. \tag{21}$$

For simplicity, we set the chemical potentials $\mu_{\rm H} = \mu_{\rm C} = \mu_{\rm S} = \mu_{\rm D} = 0$, and consider an ideal tunneling case in the following calculation, i.e., the bare tunneling rates $[\gamma_{\rm H}]_{mhc}^{m'h'c'} = [\gamma_{\rm C}]_{mhc}^{m'h'c'} = \gamma$, $[\gamma_{\rm S}]_{mhc}^{m'h'c'} = \gamma$ except $[\gamma_{\rm S}]_{100}^{000} = [\gamma_{\rm S}]_{000}^{100} = 0$, $[\gamma_{\rm D}]_{mhc}^{m'h'c'} = 0$ except $[\gamma_{\rm D}]_{100}^{000} = [\gamma_{\rm D}]_{000}^{100} = \gamma$. This means that when $\rm QD_H$ and $\rm QD_C$ are empty, $\rm QD_M$ is decoupled from reservoir D. However, if either $\rm QD_H$ or $\rm QD_C$ is occupied, $\rm QD_M$ will be decoupled from reservoir S.

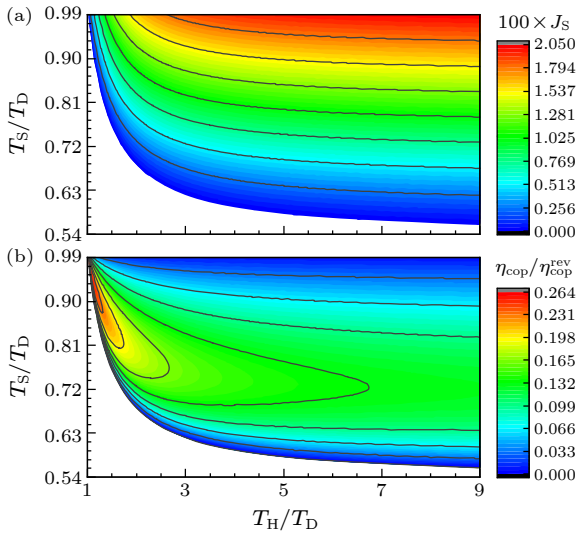

Fig. 3. (a) Cooling power $J_{\rm S}$ as a function of temperature ratios $T_{\rm S}/T_{\rm D}$ and $T_{\rm H}/T_{\rm D}$. (b) COP ratio $\eta_{\rm COP}/\eta_{\rm COP}^{\rm rev}$ as a function of temperature ratios $T_{\rm S}/T_{\rm D}$ and $T_{\rm H}/T_{\rm D}$. Other parameters are $U_{\rm MH}/\gamma = 0.2$, $U_{\rm MC}/\gamma = 2$, $U_{\rm HC}/\gamma = 0.5$, $k_{\rm B}T_{\rm D}/\gamma = 1$, $\varepsilon_{\rm H} = \varepsilon_{\rm C} = \varepsilon_{\rm M} = 0$.

Using Eqs. (4) and (19)–(20) we can plot cooling power $J_{\rm S}$ and COP ratio $\eta_{\rm COP}/\eta_{\rm COP}^{\rm rev}$ as functions of temperature ratios $T_{\rm S}/T_{\rm D}$ and $T_{\rm H}/T_{\rm D}$. Figure 3(a) shows that cooling power $J_{\rm S}$ is large when the temperature of the source is close to the temperature of the drain and the temperature of the hot thermal reservoir is much larger than the temperature of the drain. The cooling power increases monotonically with the increase in $T_{\rm H}$ at given $T_{\rm S}$. The lowest temperature $T_{\rm S}$ of the source, which can be cooled down, is about $T_{\rm S} \approx 0.55T_{\rm D}$ due to the $J_{\rm S} = 0$ line. Figure 3(b) shows that the COP ratio $\eta_{\rm COP}/\eta_{\rm COP}^{\rm rev}$ first increases and then decreases with the increase in $T_{\rm S}$ at a given $T_{\rm H}$. The COP ratio $\eta_{\rm COP}/\eta_{\rm COP}^{\rm rev}$ is large when $T_{\rm H} \approx 1.1T_{\rm D}$ and $T_{\rm S} \approx 0.9T_{\rm D}$, while the cooling power is rather low at these temperature values.

Figure 4(a) shows that cooling power $J_{\rm S}$ decreases linearly with the increase in charging energy $U_{\rm MH}/\gamma$ at given $U_{\rm MC}/\gamma$, while cooling power $J_{\rm S}$ first increases and then decreases with the increase in charging energy $U_{\rm MC}/\gamma$ at given $U_{\rm MH}/\gamma$. Cooling power $J_{\rm S}$ is large when $U_{\rm MH}/\gamma \to 0$ and $U_{\rm MC}/\gamma \approx 1.5$. The curves of the COP ratio $\eta_{\rm COP}/\eta_{\rm COP}^{\rm rev}$ with charging energy $U_{\rm MH}/\gamma$ and $U_{\rm MC}/\gamma$ are similar to those of cooling power $J_{\rm S}$, as shown in Fig. 4(b). The maximum COP ratio $\eta_{\rm COP}/\eta_{\rm COP}^{\rm rev}$ is at $U_{\rm MH}/\gamma \to 0$ and $U_{\rm MC}/\gamma \approx 1.8$.

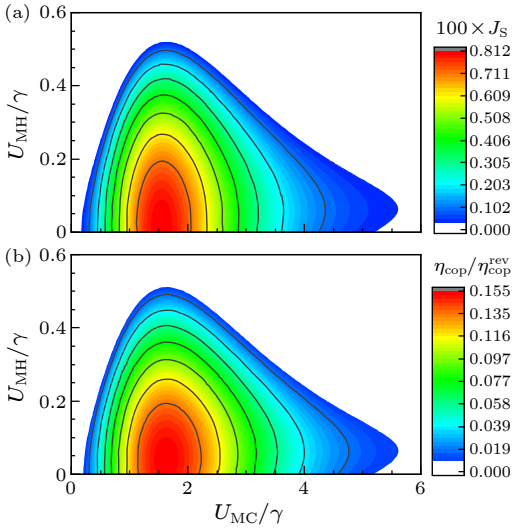

Fig. 4. (a) Cooling power $J_{\rm S}$ as a function of the charging energies $U_{\rm MH}/\gamma$ and $U_{\rm MC}/\gamma$. (b) COP ratio $\eta_{\rm COP}/\eta_{\rm COP}^{\rm rev}$ as a function of the charging energies $U_{\rm MH}/\gamma$ and $U_{\rm MC}/\gamma$. Other parameters are $k_{\rm B}T_{\rm D}/\gamma = 1$, $U_{\rm HC}/\gamma = 0.5$, $k_{\rm B}T_{\rm S}/\gamma = 0.7$, $k_{\rm B}T_{\rm H}/\gamma = 9$, $\varepsilon_{\rm H} = \varepsilon_{\rm C} = \varepsilon_{\rm M} = 0$.

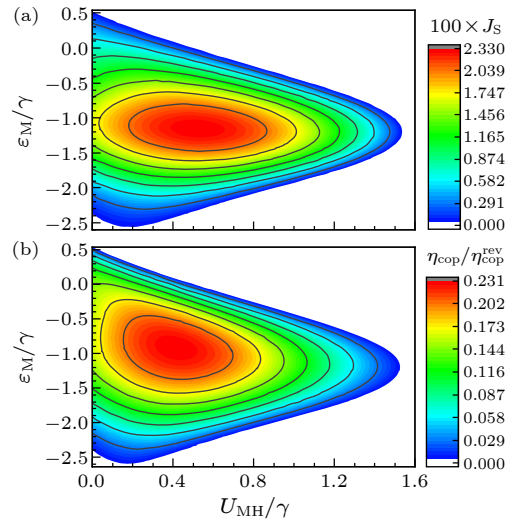

Fig. 5. (a) Cooling power $J_{\rm S}$ as a function of charging energy $U_{\rm MH}/\gamma$ and QD energy $\varepsilon_{\rm M}/\gamma$. (b) COP ratio $\eta_{\rm COP}/\eta_{\rm COP}^{\rm rev}$ as a function of charging energy $U_{\rm MH}/\gamma$ and QD energy $\varepsilon_{\rm M}/\gamma$. Other parameters are $k_{\rm B}T_{\rm D}/\gamma = 1$, $k_{\rm B}T_{\rm S}/\gamma = 0.7$, $k_{\rm B}T_{\rm H}/\gamma = 9$, $\varepsilon_{\rm H} = \varepsilon_{\rm C} = \varepsilon_{\rm M}$, $U_{\rm HC}/\gamma = 0.5$, $U_{\rm MC}/\gamma = 2$.

Figure 5(a) shows that cooling power $J_{\rm S}$ first increases

and then decreases with the increase in charging energy $U_{\rm MH}/\gamma$ at given $\varepsilon_{\rm MH}/\gamma$, while cooling power $J_{\rm S}$ first increases and then decreases with the increase in QD energy $\varepsilon_{\rm MH}/\gamma$ at a given $U_{\rm MH}/\gamma$. Cooling power $J_{\rm S}$ is large when $\varepsilon_{\rm MH}/\gamma \approx -1.3$ and $U_{\rm MH}/\gamma \approx 0.5$. The curves of the COP ratio $\eta_{\rm COP}/\eta_{\rm COP}^{\rm rev}$ with charging energy $U_{\rm MH}/\gamma$ and $U_{\rm MC}/\gamma$ are similar to those of cooling power $J_{\rm S}$, as shown in Fig. 5(b). The maximal $\eta_{\rm COP}/\eta_{\rm COP}^{\rm rev}$ appears when $U_{\rm MH}/\gamma \approx 0.4$ and $\varepsilon_{\rm M}/\gamma \approx -1$.

The second law of thermodynamics, which states that the entropy production of any macroscopic system cannot be negative, is general law. However, using the concept of Maxwell's demon one can explain the possibility of violating the second law of thermodynamics. Our four-terminal thermoelectric system can possibly be realized as Maxwell's demon using Coulomb heat drag effect. Here, we introduce Maxwell's demon based on two thermal reservoirs that can reduce the entropy of the working substance (including three coupled quantum dots, the source and the drain), without changing the energies and particles of the working substance. The condition under which Maxwell's demon neither injects nor extracts heat or energy into the working substance is $J_{\rm in} = 0$.

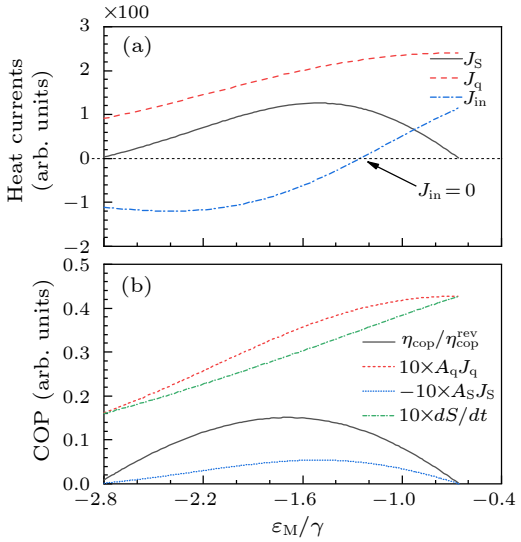

Fig. 6. (a) Cooling power $J_{\rm S}$, total heat current $J_{\rm in}$ and heat current $J_{\rm q}$ as functions of QD energy $\varepsilon_{\rm M}/\gamma$. (b) COP ratio $\eta_{\rm COP}/\eta_{\rm COP}^{\rm rev}$, entropy production rate dS/dt, $-J_{\rm S}A_{\rm S}$, and $J_{\rm q}A_{\rm q}$ as functions of QD energy $\varepsilon_{\rm M}/\gamma$. Other parameters are $U_{\rm MH}/\gamma = 1$, $U_{\rm MC}/\gamma = 2$, $U_{\rm HC}/\gamma = 0.5$, $k_{\rm B}T_{\rm D}/\gamma = 1$, $k_{\rm B}T_{\rm S}/\gamma = 0.7$, $k_{\rm B}T_{\rm H}/\gamma = 9$, $\varepsilon_{\rm H} = \varepsilon_{\rm C} = 0$.

One can see from Fig. 6(a) that our system is indeed able to realize the cooling by Coulomb heat drag effect with no net heat exchange between the thermal reservoirs and the electron reservoirs, i.e., $J_{\rm in} = 0$. The cooling driven by thermal current $J_{\rm q}$ emerges in the whole region of $-2.8 \leqslant \varepsilon_{\rm M}/\gamma \leqslant -0.6$ as long as $J_{\rm q} > 0$, regardless of the sign change and the vanishing of the total injected heat current into $\rm QD_H$ and $\rm QD_C$ from the two thermal reservoirs H and C. At $\varepsilon_{\rm M}/\gamma \approx -1.8$, i.e., $J_{\rm in} = 0$, the cooling by Coulomb heat drag effect indeed survives. In Fig. 6(b), we show that $J_{\rm S}A_{\rm S}$ is negative and $J_{\rm q}A_{\rm q}$ is positive. The entropy decrease of the working substance is compensated for by the entropy increase of the two thermal reservoirs, while the entropy of the whole four-terminal thermoelectric system is still increasing.

Our proposed device is similar to those recently realized in experiments,[35–38] in which a quantum dot generates a charge current between two reservoirs (S and D) by the rectification of thermal fluctuations in a third capacitively coupled heat reservoir. However, it is likely that the dot has a weak capacitive coupling to thermal fluctuations in its cold environment. Thus, these experimental systems have a strong similarity to the four-terminal device that we discuss. The only difference is that the source S and the drain D maintain different temperatures and the same chemical potential. We believe that our device is achievable with the technologies used in the above-mentioned works.

In summary, we have studied the cooling phenomenon by Coulomb heat drag based on three coupled quantum dots. The main results are listed as follows: (1) The dependence of cooling power $J_{\rm S}$ and COP ratio $\eta_{\rm COP}/\eta_{\rm COP}^{\rm rev}$ on the temperature ratios $T_{\rm S}/T_{\rm D}$ and $T_{\rm H}/T_{\rm D}$ for a given energy configuration shows the cooling power-COP tradeoff, i.e., the cooling power is maximum while the COP is minimum, and vice versa. By choosing appropriate parameters one can ensure that the four-terminal thermoelectric system operates at its optimal working state. (2) There is a special cooling by Coulomb heat drag effect without heat exchange between the thermal reservoirs and the electron reservoirs. (3) The four-terminal thermoelectric system we propose can possibly be realized as Maxwell's demon. Our obtained results provide some theoretical guidelines for the design and operation of practical nanoscale thermoelectric devices.

Acknowledgements. This work was supported by the National Natural Science Foundation of China (Grant No. 11875034).

References

[1] Benenti G, Casati G, Saito K, and Whitney R S 2017 *Phys. Rep.* **694** 1
[2] Sothmann B, Sánchez R, and Jordan A N 2015 *Nanotechnology* **26** 032001
[3] Jordan A N, Sothmann B, Sánchez R, and Buttiker M 2013 *Phys. Rev. B* **87** 075312
[4] Jiang J H 2014 *J. Appl. Phys.* **116** 194303
[5] Jiang J H and Imry Y 2018 *Phys. Rev. B* **97** 125422
[6] Lin Z B, Li W, Fu J, Yang Y Y, and He J Z 2019 *Chin. Phys. Lett.* **36** 060501
[7] Lin Z B, Yang Y Y, Li W, Wang J H, and He J Z 2020 *Phys. Rev. E* **101** 022117
[8] Su G Z, Zhang Y C, Cai L, Su S H, and Chen J C 2015 *Energy* **90** 1842
[9] Su H, Wang J W, Zhao Q Y, and He J Z 2016 *Sci. Sin. Technol.* **46** 1296 (in Chinese)
[10] Yang Y Y, Xu S, Li W, and He J Z 2020 *Phys. Scr* **95** 095001
[11] Yang Y Y, Xu S, and He J Z 2020 *Chin. Phys. Lett.* **37** 120502
[12] Choi Y and Jordan A N 2015 *Phys. E* **74** 465
[13] Chen L G, Ding Z M, and Sun F R 2011 *Energy* **36** 4011

[14] Shi Z C, Fu J Q W F, and He J Z 2017 *Chin. Phys. Lett.* **34** 110501
[15] Jiang J H, Entin-Wohlman O, and Imry Y 2013 *New J. Phys.* **15** 075021
[16] Li C, Zhang Y, and He J 2013 *Chin. Phys. Lett.* **30** 100501
[17] Rutten B, Esposito M, and Cleuren B 2009 *Phys. Rev. B* **80** 235122
[18] Cleuren B, Rutten B, and Van den Broeck C 2012 *Phys. Rev. Lett.* **108** 120603
[19] Shi Z C, He J Z, and Xiao Y L 2015 *Sci. Sin.-Phys. Mech. Astron.* **45** 050502 (in Chinese)
[20] Li C, Zhang Y, Wang J H, and He J Z 2013 *Phys. Rev. E* **88** 062120
[21] Li W, Fu J, Yang Y Y, and He J Z 2019 *Acta Phys. Sin.* **68** 220501 (in Chinese)
[22] Entin-Wohlman O, Imry Y, and Aharony A 2010 *Phys. Rev. B* **82** 115314
[23] Thierschmann H, S'anchez R, Sothmann B, Buhmann H, and Monlenkamp L W 2016 *C. R. Phys.* **17** 1109
[24] Wang J H, Lai Y M, Ye Z L, He J Z, Ma Y L, and Liao Q H 2015 *Phys. Rev. E* **91** 050102(R)
[25] Erdman P A, Bhandari B, Fazio R, Pekola J P, and Taddei F 2018 *Phys. Rev. B* **98** 045433
[26] Dare A M 2019 *Phys. Rev. B* **100** 195427
[27] Ren J, Zhu J X, Gubernatis J E, Wang C, and Li B 2012 *Phys. Rev. B* **85** 155443
[28] Narozhny B N and Levchenko A 2016 *Rev. Mod. Phys.* **88** 025003
[29] Yang J, Elouard C, Splettstoesser J, Sothmann B, S'anchez R, and Jordan A N 2019 *Phys. Rev. B* **100** 045418
[30] Sánchez R and Büttiker M 2011 *Phys. Rev. B* **83** 085428
[31] Thierschmann H, Sánchez R, Sothmann B, Arnold F, Hansen W, Buhmann H, and Monlenkamp L W 2015 *Nat. Nanotechnol.* **10** 854
[32] Zhang Y C, Lin G X, and Chen J C 2015 *Phys. Rev. E* **91** 052118
[33] Singha A 2020 *J. Appl. Phys.* **127** 234903
[34] Barman A, Halder S, Varshney S K, Dutta G, and Singha A 2021 *Phys. Rev. E* **103** 012131
[35] Roche B, Roulleau P, Jullien T, Jompol Y, Farrer I, Ritchie D A, and Glattli D A 2015 *Nat. Commun.* **6** 6738
[36] Hartmann F, Pfeffer P, Höfling S, Kamp M, and Worschech L 2015 *Phys. Rev. Lett.* **114** 146805
[37] Josefsson M, Svilans A, Burke A, Hoffmann E, Fahlvik S, Thelander C, Leijnse M, and Linke H 2018 *Nat. Nanotechnol.* **13** 920
[38] Prance J R, Smith C G, Griffiths J P, Chorley S J, Anderson D, Jones G A C, Farrer I, and Ritchie D A 2009 *Phys. Rev. Lett.* **102** 146602
[39] Keller A J, Lim J S, Sánchez R, Lopez R, Amasha S, Katine J A, Shtrikman H, and Goldhaber-Gordon D 2016 *Phys. Rev. Lett.* **117** 066602
[40] Whitney R S, Sánchez R, Haupt F, and Splettstoesser J 2016 *Physica E* **82** 176
[41] Fu T, Du J, Su S, Su G, and Chen J 2021 *Eur. Phys. J. Plus* **136** 1059
[42] Xi M M, Wang R Q, Lu J C, and Jiang J H 2021 *Chin. Phys. Lett.* **38** 088801
[43] Lu J C, Jiang J H, and Imry Y 2021 *Phys. Rev. B* **103** 085429
[44] Liu X, Xu S, Gao J Z, and He J Z 2022 *Acta. Phys. Sin.* **71** 190502 (in Chinese)
[45] Entin-Wohlman O, Jiang J H, and Imry Y 2014 *Phys. Rev. E* **89** 012123